lattice mechanisms. In conclusion, we note that the broadening process observed in the present study is strongly coincidental with effects associated with the one-dimensional behavior of $Fe(N_2H_5)_2(SO_4)_2$ in studies of χ_M' and C_M and may indeed be a spectroscopic reflection of such interactions. We also mention that the one-dimensional magnetic interaction in $Fe(N_2H_5)_2(SO_4)_2$ has been studied[16] using high-field Mössbauer spectroscopy and magnetization methods. For powder samples in applied fields of ~75 kG, the decoupling of antiferromagnetically coupled spins along the chain begins to occur and is complete at ca. 125 kG.

A detailed theoretical analysis of the one-dimensional behavior or the present system would attempt to correlate the observed broadening in terms of relaxation times with the magnitude of a (growing) intrachain exchange field, J, or possibly J/D for $T > T_N$. For $Fe(N_2H_5)_2(SO_4)_2$ this will be a formidable problem from a number of points of view. Previous attempts at analysis of the susceptibility[7] and heat capacity[8] data gave poor agreement and suggest that its chain behavior is intermediate to the Heisenberg and Ising extremes. This is perhaps expected for high-spin iron(II) for which considerable single-ion anisotropy is possible. In the former extreme D is neglected while in the latter the existing theory is relatively complete for $S = {}^1/_2$ (Bonner–Fisher type calculations[17]) but not for $S = 2$. As the heat capacity of $Fe(N_2H_5)_2(SO_4)$ shows a change in entropy of the spin system at T_N corresponding to $S = 2$, simple effective spin ${}^1/_2$ models are clearly inappropriate. Finally, the observation[8] $D \approx J$ adds to the mathematical intractability and makes the problem well beyond the scope and purpose of the present work.

Acknowledgment. W.M.R. acknowledges the support of the National Science Foundation, Division of Materials Research, Solid State Chemistry Program, Grant No. DMR 75-13592A01. He also acknowledges the partial support of the Research Corp. and HEW Grant No. RR 07143.

Registry No. $Fe(N_2H_5)_2(SO_4)_2$, 53091-69-3.

References and Notes

(1) L. J. De Jongh and A. R. Miedema, *Adv. Phys.*, **23**, 1 (1974).
(2) S. Foner, R. B. Frankel, W. M. Reiff, B. F. Little, and G. J. Long, *Solid State Commun.*, **16**, 159 (1975).
(3) S. Foner, R. B. Frankel, E. J. McNiff, W. M. Reiff, B. F. Little, and G. J. Long, *AIP Conf. Proc.*, **24**, 363 (1974).
(4) S. Foner, R. B. Frankel, W. M. Reiff, H. Wong, and G. Long, *AIP Conf. Proc.*, **29**, 510 (1975).
(5) P. M. Richards, R. K. Quinn, and B. Morisin, *J. Chem. Phys.*, **59**, 4474 (1973).
(6) C. K. Prout and H. M. Powell, *J. Chem. Soc.*, 4177 (1961).
(7) H. T. Witteveen and J. Reedijk, *J. Solid State Chem.*, **10**, 151 (1974).
(8) F. W. Klaaijsen, H. Den Adel, Z. Dokoupil, and W. J. Huiskamp, *Physica B + C (Amsterdam)*, **79**, 113 (1975).
(9) A. Nieuwpoort and J. Reedijk, *Inorg. Chim. Acta*, **7**, 323 (1973).
(10) G. M. Bancroft, A. G. Maddock, W. K. Ong, R. H. Prince, and A. J. Stone, *J. Chem. Soc. A*, 1966 (1967).
(11) J. Van Dongen Torman, R. Jagannathan, and J. M. Trooster, *Hyperfine Interact.*, **1**, 135 (1975).
(12) T. C. Gibb and N. N. Greenwood, "Mossbauer Spectroscopy", Chapman and Hall, London, 1971.
(13) V. Petrouleas, *Solid State Commun.*, **15**, 1097 (1974).
(14) M. Blume, *Phys. Rev. Lett.*, **18**, 305 (1967).
(15) M. Blume and J. A. Tjon, *Phys. Rev.*, **165**, 446 (1968).
(16) W. M. Reiff, H. Wong, S. Foner, and R. B. Frankel, *Inorg. Chem.*, in press.
(17) J. C. Bonner and M. E. Fisher, *Phys. Rev. A*, **135**, 640 (1964).

Contribution from the Lash Miller Chemistry Laboratory and Erindale College, University of Toronto, Toronto, Ontario, Canada

Titanium Hexacarbonyl, $Ti(CO)_6$, and Titanium Hexadinitrogen, $Ti(N_2)_6$. 1. Synthesis Using Titanium Atoms and Characterization by Matrix Infrared and Ultraviolet–Visible Spectroscopy

R. BUSBY, W. KLOTZBÜCHER, and G. A. OZIN*

Received July 8, 1976 AIC60500A

The matrix cocondensation reactions of Ti atoms with CO and N_2 either pure or diluted with the inert gases at 10–15 K are investigated for the first time by infrared and ultraviolet–visible spectroscopy. Ti and CO concentration experiments, matrix variations, warm-up studies, and comparisons with $V(CO)_6$ and $Cr(CO)_6$ formed in similar V/CO, Cr/CO matrix reactions provide convincing evidence that the green, highest stoichiometry product of the Ti/CO reaction is titanium hexacarbonyl, $Ti(CO)_6$, the first example of a binary titanium carbonyl complex. The corresponding data for the reddish-yellow, highest stoichiometry product of the Ti/N_2 reaction resemble closely those obtained for $Ti(CO)_6$ as well as those available for the novel compounds $V(N_2)_6$ and $Cr(N_2)_6$, arguing in favor of a titanium hexadinitrogen complex, $Ti(N_2)_6$. Trends in ν_{CO}, ν_{NN}, and $10Dq$ for the series $M(CO)_6$ and $M(N_2)_6$ (M = Ti, V, or Cr) support the $Ti(CO)_6/Ti(N_2)_6$ assignment and are discussed in some detail. The infrared data for $Ti(CO)_6$ and $Ti(N_2)_6$ indicate that both complexes are closely related structurally and subject to a Jahn–Teller distortion. The 40-cm^{-1} splitting observed for the T_{1u} ν_{CO} stretching mode in solid CO is retained in Ar, Kr, and Xe matrices. Both components of this split degeneracy yield linear Buckingham plots, which supports the designation of an inherent molecular distortion for $Ti(CO)_6$ rather than a matrix effect. However, the magnitude of the distortion is probably quite small, as the electronic spectra of $Ti(CO)_6$ and $Ti(N_2)_6$ display the gross features expected for low-spin d^4 octahedral complexes.

Introduction

At 10–70 K the reaction of titanium atoms and benzene yields the electron-rich, 16-electron, red complex bis(benzene)titanium(0), a long-sought-after molecule from a synthetic and catalytic point of view.[1] Apart from this work, little else is known about the reactivity of the early transition elemental vapors toward other reactive partners. Recently we turned our attention to the more fundamental question as to the fate of these metals when cocondensed at low temperatures in the presence of a nonreactive partner and have succeeded in synthesizing and characterizing for the first time relatively large amounts of Sc_2,[2] Ti_2,[2] V_2,[3] and Cr_2.[4]

In view of the direct syntheses of the 17- and 18-electron systems $V(CO)_6$[5]/$(C_6H_6)_2V$[6] and $Cr(CO)_6$[7]/$(C_6H_6)_2Cr$[8] by metal vapor cocondensation techniques, it occurred to us by analogy with the 16-electron $(C_6H_6)_2Ti$ complex that the 16-electron $Ti(CO)_6$ complex would be a worthwhile synthetic goal. Furthermore, the recently established 17- and 18-electron

hexadinitrogen complexes $V(N_2)_6$[9] and $Cr(N_2)_6$[10a,b] stimulated our search for the 16-electron $Ti(N_2)_6$ analogue. Experimentally, both of these goals were realized and what follows is a detailed account of the synthesis and spectroscopic characterization of $Ti(CO)_6$ and $Ti(N_2)_6$.

Experimental Section

Our experimental techniques and apparatus have been described elsewhere.[11] The crucial aspect of the method involves the precise control and measurement of the rate of metal atom deposition onto the cooled optical window. This was achieved with the aid of a quartz crystal microbalance incorporated into the furnace–cryostat assembly.[12]

Monatomic Ti was generated by directly heating a thin filament (0.010 in.) of the metal (99.999%) which was supplied by McKay, New York, N.Y. Research grade $^{12}C^{16}O$, $^{14}N_2$, Ar, Kr, and Xe (99.99%) were supplied by Matheson of Canada. In the infrared experiments, matrices were deposited on either a NaCl or CsI optical window cooled to 10–12 K by means of an Air Products Displex closed cycle helium refrigerator. Infrared spectra were recorded on a Perkin-Elmer 621 spectrophotometer. UV–visible spectra were recorded on a standard Unicam SP8000 instrument in the range 200–700 nm, the sample being condensed onto a NaCl optical plate cooled to 10–12 K.

Results

(A) The Titanium Atom–Carbon Monoxide Reaction. (1) Infrared Experiments. By analogy with the results obtained from V/CO[5] and Cr/CO[7] matrix cocondensation reactions which provide a direct synthetic pathway to $V(CO)_6$ and $Cr(CO)_6$, one would anticipate that similar reactions between atomic Ti and CO or concentrated CO–inert gas mixtures might lead to the elusive $Ti(CO)_6$ complex.

Before discussing the details of these experiments, certain aspects of our methodology should be clarified. Past experiences with M/CO matrix reactions[5,7,13] lead us to anticipate that the highest stoichiometry product in the Ti/CO reaction should be generated in either pure CO or concentrated CO–inert gas mixtures. The use of the highly rigid and polarizable matrix gases Kr and Xe is expected to minimize the facile matrix diffusion and dimerization processes commonly observed for the first transition series metal atoms.[2-4,14] However, the advantages gained in Kr and Xe tend to be counterbalanced to some extent by their higher quenching efficiency and resulting isolation of *lower* binary carbonyl fragments. This difficulty can often be eliminated by employing warm (20–25 K) depositions which enhance the formation of the highest stoichiometry product.

A final point that should be mentioned involves the physical size and shape of the reaction product(s) relative to the dimensions and symmetry of the available matrix sites. Experience has shown[5] that trapping of $M(CO)_6$ complexes requires at least two adjacent substitutional sites in the fccub lattices of the solid inert gases. Moreover, the packing requirements for such complexes in the matrix cage enforce site symmetries below that of cubic to tetragonal.[5] In solid CO this situation can be further aggravated by the lower substitutional site symmetry of C_2.[15] Consequently, splitting of some or all of the vibrational modes can be expected and careful examination of the reaction product(s) in a variety of matrix environments with different concentration, deposition, and annealing histories is a prerequisite for making meaningful vibrational and structural assignments.

With these points in mind we begin by discussing the infrared spectrum obtained after depositing Ti atoms with CO/Kr $\simeq$ 1/10 mixtures at 20 K (Figure 1 and Table I). Low metal concentrations Ti/Kr $\simeq 1/10^5$ were employed to minimize complications arising from matrix diffusion and aggregation effects.[14]

The main feature of this spectrum is the appearance of two CO stretching modes at 1985 and 1947 cm^{-1}. These absorptions maintain the same relative intensities throughout the deposition and warm-up processes. Moreover, they continue to be the major absorptions after a series of warm-up experiments in the range 10–30 K, during which time the weaker absorptions, marked with an asterisk in Figure 1, gradually diminish in intensity and eventually disappear, concomitant with the growth of a broad, partially resolved band (marked with a double asterisk in Figure 1B) centered at roughly 2012 cm^{-1}. Ti concentration experiments demonstrate that the absorbance of the band at 2012 cm^{-1} relative to the 1985/1947 cm^{-1} doublet is metal dependent and, by analogy with the $V(CO)_6/V_2(CO)_{12}$[5] and similar studies,[14] is best ascribed to a binuclear or higher titanium cluster carbonyl species. On the other hand, the bands marked with an asterisk are not metal dependent and become more prominent on employing lower temperature depositions (6–12 K) and/or higher dilution experiments (CO/Kr $\simeq$ 1/50).

These results serve to identify the species giving rise to the 1985/1947 cm^{-1} doublet to be the highest stoichiometry, mononuclear titanium carbonyl (labeled VI) in the Ti/CO system. The lines marked with an asterisk in Figure 1 are clearly associated with lower titanium carbonyl fragments than VI and are not of direct interest in this study.

Similar results were obtained in CO/Xe $\simeq$ 1/10 mixtures at 20–25 K, where the strongest feature was a doublet at 1982/1944 cm^{-1} which, from its warm-up behavior, can be associated with a single species. The close resemblance to the Kr data strongly suggests that it can be assigned to the same species VI, having experienced a small matrix-induced frequency shift of 3 cm^{-1} (see later for details).

Particularly noteworthy in these Xe matrix experiments was the complete absence of the feature observed around 2012 cm^{-1} in Kr, supporting the view that it is probably associated with

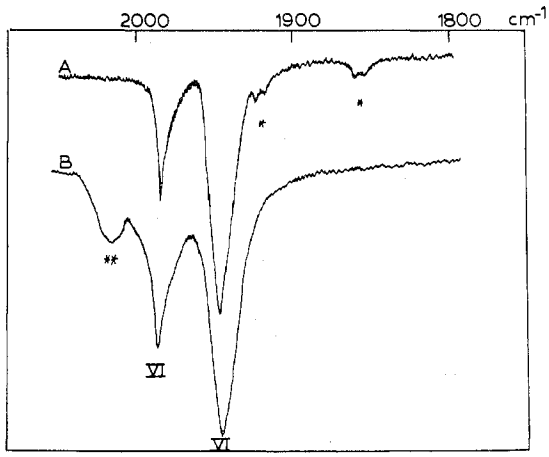

Figure 1. The matrix infrared spectrum of the products formed when Ti atoms are cocondensed with CO/Kr $\simeq$ 1/10 mixtures (Ti/Kr $\simeq 1/10^5$) (A) at 20 K and (B) after warm-up to 30 K. The lines marked with the Roman numeral VI refer to the CO stretching modes of $Ti(CO)_6$, those marked with an asterisk to lower carbonyls $Ti(CO)_n$ (where $n < 6$), and those with a double asterisk to a $Ti_x(CO)_y$ cluster where x is probably 2.

Table I. Infrared Spectroscopic Data for $Ti(CO)_6$ in CO, Ar, Kr, and Xe Matrices

Matrix support	ν_{CO}(obsd), cm^{-1}
CO[a]	1985, 1953, 1945
Ar[b]	1987, 1950
Kr[b]	1985, 1947
Xe[b]	1982, 1944

[a] Depending on the deposition conditions, each of these CO stretching modes can experience a further matrix splitting to yield absorptions centered at 1986, 1979/1955, 1950, 1945, 1932 cm^{-1}. [b] CO/M $\simeq$ 1/10 mixtures used where M = Ar, Kr, or Xe.

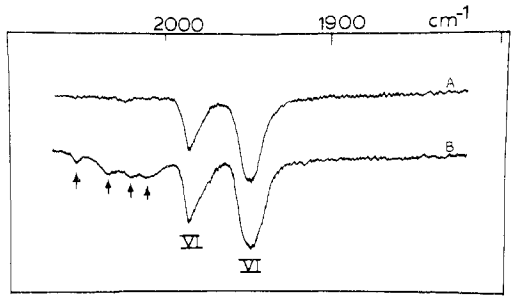

Figure 2. The same as Figure 1 except CO/Ar ≃ 1/10 mixtures, deposited at 10–12 K, were used. Lines marked with an arrow refer to $Ti_x(CO)_y$ where x is probably 2.

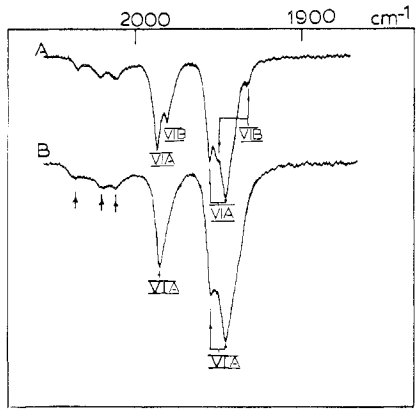

Figure 3. The same as Figure 1 except pure CO matrices were used at 10–12 K. (A) and (B) show the sensitivity of the spectrum of $Ti(CO)_6$ to deposition conditions where VIA and VIB refer to different matrix sites of $Ti(CO)_6$. Lines marked with an arrow refer to $Ti_x(CO)_y$, where x is probably 2.

a $Ti_x(CO)_y$ cluster complex.[14]

The results in CO/Ar ≃ 1/10 mixtures deposited at 10–12 K generally support the conclusions drawn from the Kr and Xe results. As before, the major spectral features are two CO stretching modes at 1987/1950 cm^{-1} (Figure 2A, Table I) which, from their concentration and annealing behavior, can confidently be ascribed to species VI. The absence of lower carbonyl fragments on deposition attests to the more highly mobile nature of Ar at 10–12 K compared to Kr and Xe at 20–25 K. By warming the matrix to 30–40 K or by increasing the Ti deposition rate or deposition temperature, absorptions in the region 2058, 2035, 2024, and 2011 cm^{-1} could be resolved and can be seen to grow in relative to those of species VI (Figure 2B). As described earlier, this behavior is that expected for $Ti_x(CO)_y$ cluster formation, where x is probably 2.

The infrared spectroscopic results obtained in pure CO matrices were qualitatively similar to those in Ar, Kr, and Xe. A typical spectrum for Ti/CO ≃ $1/10^5$ deposited at 10–12 K is shown in Figure 3A and once again shows two major absorptions centered at 1985.5/1943.5 cm^{-1} (with substantial superimposed fine structure). To begin with, resolution of the component fine structure on the 1985.5/1943.5 cm^{-1} doublet was particularly sensitive to the rate and temperature of the matrix gas deposition and thermal annealing history of the matrix. Depending on the conditions chosen, these CO stretching modes could appear as a well-resolved doublet/quartet structure at 1986, 1979/1955, 1950, 1945, 1932 cm^{-1} (Figure 3A) or a broadened singlet–doublet at roughly 1985/1953, 1945 cm^{-1} (Figure 3B). However, the gross features of this spectrum are similar to those found in Ar, Kr, and Xe for species VI, and the fine splittings are not unexpected in view of the lower substitutional site symmetry of solid

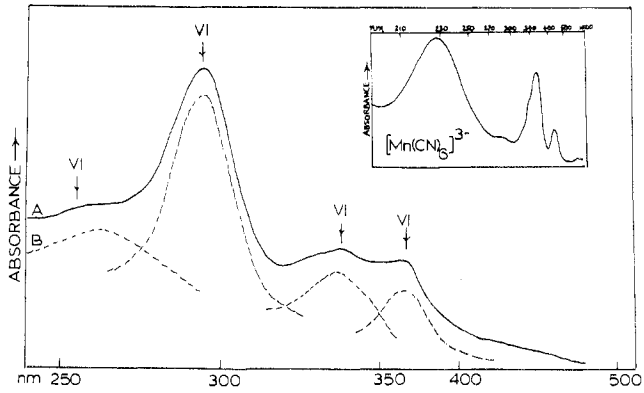

Figure 4. (A) The matrix UV–visible spectrum of $Ti(CO)_6$ formed when Ti atoms are cocondensed with pure CO (Ti/CO ≃ $1/10^5$) at 10–12 K. (B) The curve-resolved spectrum of (A). (C) The UV–visible spectrum of $[Mn(CN)_6]^{3-}$ in 1.86–3.54 M perchloric acid.[19] (VI refers to the absorptions of $Ti(CO)_6$.)

CO (see later).[15] Of greatest significance is the fact that the roughly 37 cm^{-1} splitting between the two major lines of compound VI *is retained* in Ar, Kr, Xe, and CO matrices on deposition and after annealing in the temperature range 10–40 K.

Experiments with long deposition times in pure CO matrices produced weak low-frequency modes at 600, 545, 440, and 360 cm^{-1}, associated with compound VI. These are clearly related to νTi–C stretching and $\delta\angle$TiC≡O deformational motions of the molecule (see Table IV).

A final point concerning the Ti/CO cocondensations relates to the Ti concentration dependence of the infrared spectra. Under conditions which favor atom reactions, Ti/CO ≃ $1/10^5$, the only observable features are those of compound VI around 1985/1953, 1945 cm^{-1}. However, on increasing Ti/CO to ≃ $1/10^3$, three new lines begin to grow in at roughly 2010, 2020, and 2032 cm^{-1} relative to the doublet absorption of VI. By analogy with the Ar, Kr, and Xe data and the similar behavior observed in the V/CO system,[5] these lines are probably best associated with a binuclear $Ti_2(CO)_n$ carbonyl.[14] Unlike the V/CO reaction in which divanadium dodecacarbonyl $(OC)_5V(\mu\text{-}CO)_2V(CO)_5$ with bridging CO groups could be identified,[5] the binuclear product $Ti_2(CO)_n$ in pure CO matrices displayed no evidence of bridging CO groups.

(2) Ultraviolet–Visible Experiments. Examination of the ultraviolet–visible spectrum of compound VI in pure CO matrices under identical conditions to those used in the infrared experiments (Ti/CO ≃ $1/10^5$) shows the presence of at least two high-energy bands centered at 263 and 295 nm and two lower energy bands at 336 and 368 nm (Figure 4A). The absence of the most intense Ti atom resonance absorptions[2] under the conditions of this experiment indicates that the Ti/CO cocondensation reaction proceeds to completion even at 10–12 K (cf. V/CO → $V(CO)_6$;[5] Cr/CO → $Cr(CO)_6$[7]) and should be contrasted with the results for the Ti/N_2 reaction, to be described later. Warm-up experiments in the range 10–40 K confirm that the four aforementioned absorptions can be assigned to a single species, namely, compound VI.

Discussion of Results. The infrared and ultraviolet–visible data for compound VI, when compared with the available data for the products of the analogous V/CO[5] and Cr/CO[7] matrix reactions, are best rationalized in terms of a slightly distorted $Ti(CO)_6$ complex.

Let us formalize the data. To begin with, an octahedral $Ti(CO)_6$ complex would be expected to be a low-spin, d^4 system, with a $^3T_{1g}(t_{2g}^4)$ electronic ground state, and is anticipated to be weakly Jahn–Teller unstable. Assuming that a small D_{4h} tetragonal distortion exists for $Ti(CO)_6$ (similar arguments apply to a D_{3d} trigonal distortion), then one can

Table II. Matrix-Induced Frequency Shifts for $Ti(CO)_6$ in Solid Ar, Kr, and Xe

Matrix	ν_{CO}(obsd),[a] cm^{-1}		$\Delta\nu$, cm^{-1}		ν,[b] cm^{-1}		$\Delta\nu/\nu \times 10^{-3}$		
	I	II	I	II	I	II	I	II	$(\epsilon' - 1)^a/(2\epsilon' + 1)^c$
Ar	1987	1950	3	4	1988.5	1952.0	1.509	2.049	0.148
Kr	1985	1947	5	7	1987.5	1950.5	2.516	3.589	0.185
Xe	1982	1944	8	10	1986.0	1949.0	4.208	5.131	0.221
Gas[d]	1990	1954							

[a] I and II refer to the two-component CO stretching modes assigned to $Ti(CO)_6$. [b] Arithmetic mean of ν_{gas} and ν_{matrix} frequencies. [c] ϵ'(20 K): Ar = 1.63, Kr = 1.88, Xe = 2.19 (see H. Hallam, "Vibrational Spectra of Trapped Species", Wiley, New York, N.Y., 1974). [d] Hypothetical gas-phase frequency obtained by extrapolation to $\alpha = 0$ in polarizability frequency plot of Figure 5.

Chart I

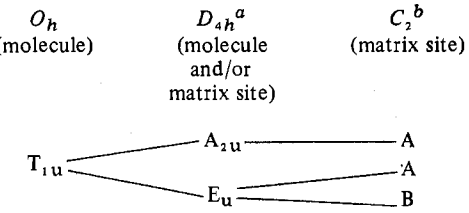

[a] Note that placing an O_h $M(CO)_6$ molecule in two adjacent substitutional sites of a fccub inert gas lattice also enforces a tetragonal site symmetry on the entrapped guest.[5] [b] Note that the substitutional site symmetry of solid CO is C_2.[15]

expect this to be manifested in the removal of the degeneracy of the infrared-active T_{1u} νCO stretching mode as indicated in the correlation diagram in Chart I. The substantial 36–39 cm^{-1} splitting between the two CO stretching modes of $Ti(CO)_6$ in Ar, Kr, and Xe matrices is considerably larger than the 6–9-cm^{-1} splittings observed for $V(CO)_6$[5] and $Cr(CO)_6$[7] in similar matrix environments. This leads one to believe that the removal of the T_{1u} νCO degeneracy in $Ti(CO)_6$ is reflecting a genuine molecular distortion of a more substantial nature than that observed for $V(CO)_6$, the latter being of the same order of magnitude as the matrix site effect ascribed to $Cr(CO)_6$. In CO, further reduction in site symmetry to C_2 (see correlation scheme) must be invoked.

Additional support for the proposed $Ti(CO)_6$ molecular distortion stems from the *linear* polarizability–frequency plot (Figure 5) for the two CO stretching modes in Ar, Kr, Xe, and CO matrices and the approximately constant 36–39-cm^{-1} splitting between these two modes. Moreover, the linearity and parallel behavior of the resulting Buckingham[16] plots (Figure 6 and Table II) for both components of the νCO doublet splitting of $Ti(CO)_6$ lend credence to the idea[17] that the observed molecular distortion is electronic in origin rather than the outcome of a specific $Ti(CO)_6$···matrix interaction.

Up to this point we have tacitly assumed that compound VI is $Ti(CO)_6$ without really justifying our reasons for eliminating $Ti(CO)_5$ or $Ti(CO)_7$ as possible alternatives. Three observations strongly suggest that the alternative formulations need not be seriously considered. To begin with, consider the monotonically increasing trend in the CO stretching frequencies for $Ti(CO)_6$, $V(CO)_6$, and $Cr(CO)_6$[23] shown in Figure 7. This is exactly the behavior that one would have predicted for a series of hexacarbonyl complexes in which the effective nuclear charge gradually increases, as is found on passing from (d^4) $Ti(CO)_6$ to (d^5) $V(CO)_6$ to (d^6) $Cr(CO)_6$. If, on the other hand, we assume that VI is D_{3h} $Ti(CO)_5$, which could produce an infrared spectrum of the type observed, then similar νCO frequency comparisons with the available data for $V(CO)_5$[18] and $Cr(CO)_5$[7] give the reverse trend to that expected, that is, νCO of VI is higher than that of $V(CO)_5$ and $Cr(CO)_5$ (Figure 8).

A second important clue relates to the striking resemblance of the ultraviolet–visible spectrum of VI to that of the low-spin, d^4 $[Mn(CN)_6]^{3-}$ complex[19,20] shown in Figure 4 for the purposes of comparison. The similarity between these two sets

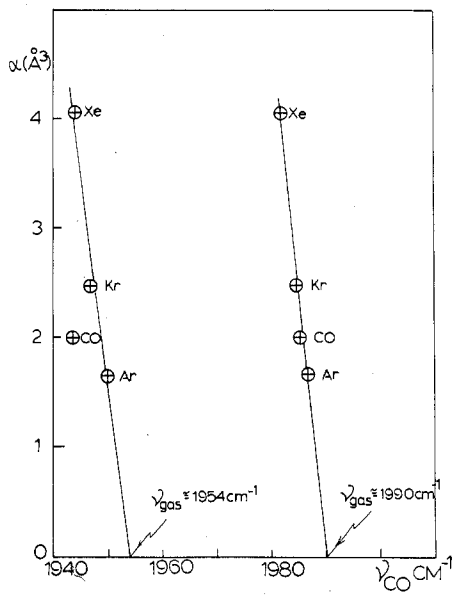

Figure 5. Graphical representation of the effect of the matrix polarizability on the doublet splitting of $Ti(CO)_6$ in Ar, Kr, Xe, and CO matrices.

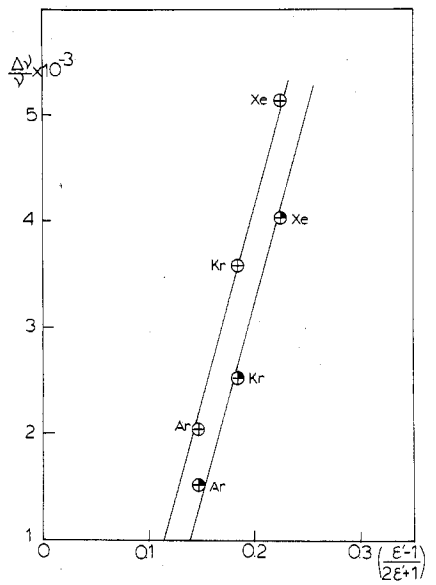

Figure 6. Buckingham plot for both components of the doublet splitting of $Ti(CO)_6$ in Ar, Kr, and Xe matrices.

of electronic data lends support to the low-spin, d^4 $Ti(CO)_6$ assignment for VI. By using theoretical arguments outlined in detail in paper 2 of this series[10a] for the analysis of the electronic spectrum of the low-spin d^4 $Ti(CO)_6$ complex (assuming a small distortion from O_h symmetry) we arrive at $10Dq$ = 28 255 cm^{-1} for the crystal field splitting energy of $Ti(CO)_6$. This value is compared with $10Dq$ for $V(CO)_6$ and $Cr(CO)_6$ as shown in Figure 9 and shows a smooth, monotonic

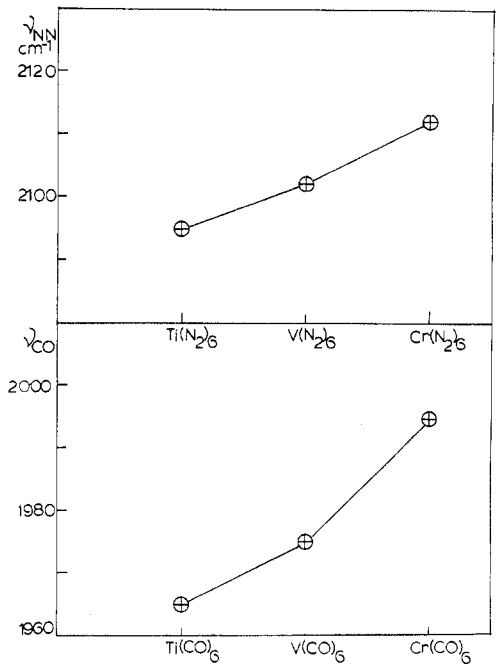

Figure 7. Graphical representation of the CO stretching frequencies for $M(CO)_6$ and $M(N_2)_6$ (where M = Ti, V, or Cr). For consistency, the average CO or NN stretching frequency for the doublet splitting has been used in this figure.

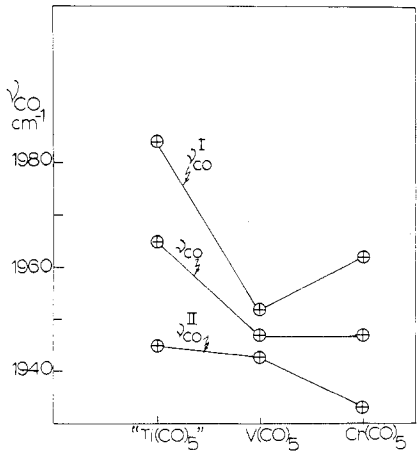

Figure 8. Graphical representation of the CO stretching frequencies for compounds VI, $V(CO)_5$, and $Cr(CO)_5$. The two observed CO stretching frequencies for the pentacarbonyls, ν_{CO}^{I} and ν_{CO}^{II}, as well as their respective arithmetic mean frequency $\bar{\nu}_{CO}$ are plotted in this figure and compared with the corresponding values for VI.

increase on passing from $Ti(CO)_6$ to $V(CO)_6$ to $Cr(CO)_6$. A similar trend has been observed[21] for the hexacyanide complexes $Ti(CN)_6^{3-}$, $V(CN)_6^{3-}$, and $Cr(CN)_6^{3-}$, that is, $10Dq$ increases as the number of d electrons increases in both the $M(CN)_6^{3-}$ and $M(CO)_6$ complexes. This trend implies that the increased destabilization of the e_g^* orbital set on passing from Ti to Cr through more effective M–C σ bonding more than offsets the expected destabilization of the t_{2g} orbital set through less effective M–C π bonding.

Summarizing up to this point, we can state that the vibrational and electronic properties of compound VI, vis-à-vis crystal field splitting energies, carbonyl stretching, nuclear charge correlations with respect to $V(CO)_6$ and $Cr(CO)_6$ are consistent with those expected for a low-spin, d^4 hexacarbonyl complex, $Ti(CO)_6$.

(B) The Titanium Atom–Dinitrogen Reaction. (1) Ultraviolet–Visible Experiments. We chose first to discuss the UV–visible spectroscopic data for the Ti/N_2 matrix reaction

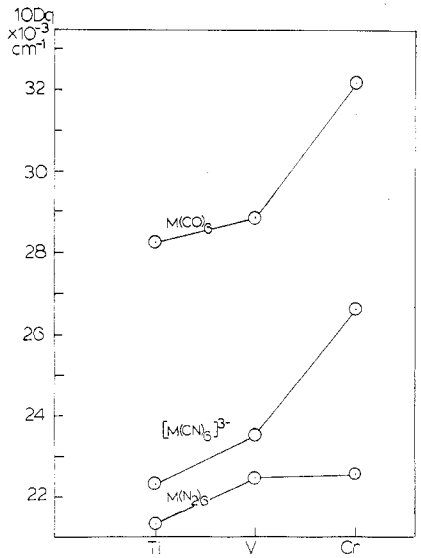

Figure 9. Graphical representation of $10Dq$ for $M(CO)_6$, $M(N_2)_6$, and $[M(CN)_6]^{3-}$ (where M = Ti, V, or Cr). See ref 10a for the details of the $10Dq$ calculations.

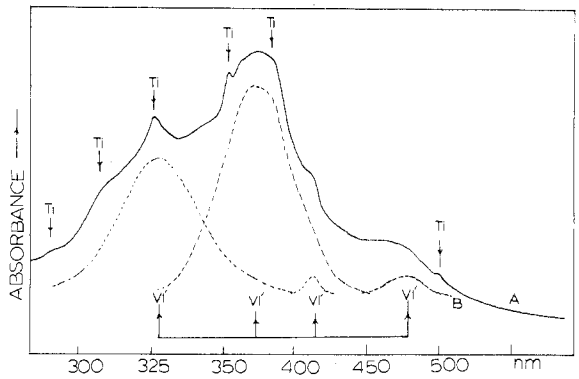

Figure 10. The matrix UV–visible spectrum of the products formed when Ti atoms are cocondensed with pure N_2 ($Ti/N_2 \simeq 1/10^5$) (A) at 16 K and (B) the curve-resolved spectrum of (A). Atomic Ti resonance absorptions are indicated.

Table III. Optical Data for Matrix-Isolated $Ti(CO)_6$ and $Ti(N_2)_6$

$Ti(CO)_6$[a]		$Ti(N_2)_6$[b]		Δ[c],	Tentative assignment[d]
nm	cm^{-1}	nm	cm^{-1}	cm^{-1}	(d^4, low spin)
263	38023	327	30581	7442	CT 2(CO), $t_{2g} \rightarrow t_{2u}$
295	33898	374	26738	7160	CT 1(CO), $t_{2g} \rightarrow t_{1u}$
336	29762	415	24096	5666	d–d; $^3T_{1g} \rightarrow {}^3A_{1g}, {}^3A_{2g}$
368	27174	480	20833	6341	d–d; $^3T_{1g} \rightarrow {}^3E_g, {}^3T_{1g}, {}^3T_{2g}$

[a] Frequencies refer to pure CO matrices. [b] Frequencies refer to pure N_2 matrices. [c] Δ refers to the difference between the corresponding absorptions of $Ti(CO)_6$ and $Ti(N_2)_6$. [d] CT refers to charge transfer. (See ref 10a for details of these assignments and $10Dq$ calculations.)

because of a fundamental difference from that of the corresponding Ti/CO reaction.

Thus, when Ti atoms are cocondensed with pure N_2 under conditions of high metal dilution ($Ti/N_2 \simeq 1/10^5$) at 10–12 K, the UV–visible spectrum shows the isolation of essentially Ti atoms.[2] On annealing the matrix at 30 K, the atomic spectrum gradually diminishes in intensity, leaving behind a yellowish-red matrix which displays weak absorptions attributable to a molecular species. This same molecular spectrum can be generated directly by performing the initial Ti/N_2 cocondensation reaction at 16 K (Figure 10A). The curve-resolved spectrum (Figure 10B) shows the presence of two high-energy peaks centered at 327 and 374 nm as well as two weaker, low-energy bands at 415 and 480 nm. Careful

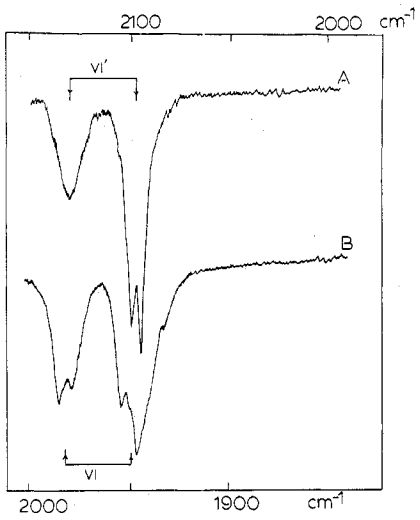

Figure 11. The matrix infrared spectra of the products formed when Ti atoms are cocondensed with (A) pure N_2 ($Ti/N_2 \simeq 1/10^5$) at 16 K (showing VI′ = $Ti(N_2)_6$) and (B) pure CO ($Ti/CO \simeq 1/10^5$) at 10–12 K (showing VI = $Ti(CO)_6$). Note that the frequency scale of spectrum (B) has been shifted with respect to (A) to emphasize the similarity between the two sets of data.

warm-up studies show that these four absorptions belong to a single species which we shall label VI′.

This molecular spectrum, aside from a *red* frequency shift of roughly 5500–7500 cm^{-1} on the observed lines (Table III), is qualitatively identical to that observed for the corresponding Ti/CO reaction and suggests an a priori assignment to $Ti(N_2)_6$.

The isolation of either metal atoms or metal complexes in the Ti/N_2 reaction parallels the results previously obtained for the V/N_2[9] and Cr/N_2[10] reactions and implies that a very delicate balance must exist between the activation energy for complexation and the thermal energy available at the reaction zone, the latter being intimately related to the temperature at which the deposition is conducted. The fact that the corresponding Ti/CO, V/CO, and Cr/CO reactions proceed to completion even at 10–12 K means that complex formation for the carbonyls compared to the respective dinitrogen complexes is a more facile process. Whether this is because of a lower energy of activation or a higher heat of reaction for the carbonyls in the reaction zone, or both, remains to be ascertained.

(2) Matrix Infrared Experiments. The corresponding Ti/N_2 matrix infrared experiments were performed with 16 K depositions in order to optimize the yield of compound VI′. Figure 11A shows a typical infrared spectrum obtained under these conditions where two major bands can be seen in the NN stretching region at 2131/2100, 2095 cm^{-1}. For the purposes of comparison, the spectrum of $Ti(CO)_6$ is included in Figure 11B but on a shifted frequency scale. The resemblance between these two infrared spectra is remarkable, both in terms of the splitting of the major doublet (~34 cm^{-1} for VI′ compared to ~38 cm^{-1} for VI) and the fine structure on the strongest line (~5 cm^{-1} for VI′ compared to ~8 cm^{-1} for VI).

Warm-up experiments were performed in the temperature range 10–30 K and showed a gradual diminution in the intensities of the NN stretching modes at 2131/2100, 2095 cm^{-1} at approximately the same rate, indicating that they are all associated with a single species VI′.[24]

By using long deposition times in pure N_2 matrices, low-frequency modes associated with compound VI′ were observed at 700, 485, and 332 cm^{-1} and are compared in Table IV with the corresponding modes of $Ti(CO)_6$. These are clearly related to νTi–N stretching and $\delta\angle$Ti N≡N deformational motions of VI′.

Table IV. Low-Frequency Infrared Modes for Matrix-Isolated $Ti(CO)_6$ and $Ti(N_2)_6$

$Ti(CO)_6$,[a] cm^{-1}	Tentative assignment[c]	$Ti(N_2)_6$,[b] cm^{-1}	Tentative assignment[c]
600	$\delta\angle$TiC≡O	700	$\delta\angle$TiN≡N
545	$\delta\angle$TiC≡O		
440	$\delta\angle$TiC≡O	485	$\delta\angle$TiN≡N
360	νTi–C	332	νTi–N

[a] Recorded in solid CO. [b] Recorded in solid N_2. [c] These assignments are based on comparisons with binary carbonyls (L. H. Jones, "Inorganic Vibrational Spectroscopy", Vol. 1, Marcel Dekker, New York, N.Y., 1971), binary dinitrogen complexes (see, for example, W. Klotzbücher and G. A. Ozin, *J. Am. Chem. Soc.*, 97, 2672 (1975)), and nitrogen isotope studies of $[Ru(NH_3)_5(^nN^mN)]^{2+}$ (where $n, m = 14$ or 15; S. Pell, R. H. Mann, H. Taube, and J. N. Armor, *Inorg. Chem.*, 13, 479 (1974), and references therein). In all carbonyl and dinitrogen complexes studied to date, low-frequency absorptions in the region 700–300 cm^{-1} have been ascribed to $\delta\angle$MCO, νM–C, $\delta\angle$MNN, and νM–N modes, respectively. Invariably the deformational modes have been assigned at higher frequencies than the metal–ligand stretching modes and in the above table of tentative assignments we have adopted this same procedure.

Chart II

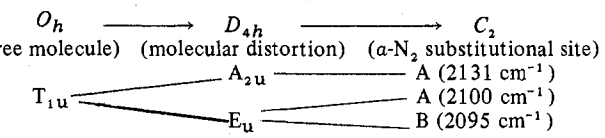

The similarity existing between the electronic and vibrational data for $Ti(CO)_6$ and VI′ strongly suggests that $Ti(N_2)_6$, probably with a small distortion from regular octahedral symmetry, is the major product of the Ti/N_2 (16 K) cocondensation reaction.

In an α-N_2 lattice which, like CO, also has a C_2 substitutional site symmetry, the splittings observed in the NN stretching region for $Ti(N_2)_6$ can be rationalized as in Chart II.

Using arguments similar to those delineated earlier for $Ti(CO)_6$, we have correlated the νNN stretching frequency and estimated ligand field splitting energy ($10Dq$) for the proposed $Ti(N_2)_6$ complex with the corresponding values for the known complexes $V(N_2)_6$[9] and $Cr(N_2)_6$,[10a] as shown in Figures 7 and 9. The monotonically increasing trend in both the νNN and $10Dq$[25] values with increasing nuclear charge in the series $Ti(N_2)_6$, $V(N_2)_6$, $Cr(N_2)_6$ is a most convincing demonstration of the validity of our $Ti(N_2)_6$ assignment.[10a] Moreover, the crystal field splitting energy of roughly 21 370 cm^{-1} for $Ti(N_2)_6$ compared to 28 255 cm^{-1} for $Ti(CO)_6$ shows that N_2 is a relatively weak ligand compared to CO.

(C) Thermal Stability Studies. Matrix warm-up and boil-off techniques were used to try to establish the thermal stabilities of $Ti(CO)_6$ and $Ti(N_2)_6$ and hence their useful working ranges for further chemical syntheses. In the case of the "green" $Ti(CO)_6$ complex, synthesized in pure CO matrices, one observes a gradual color change to a reddish-brown material at about 40–50 K as the CO lattice begins to break up. The infrared spectrum of this reddish-brown residue was recorded in the presence of a small pressure of CO but showed no evidence for coordinated CO groups. Moreover, this material could be retained on the optical window up to room temperature and remained unchanged when air was admitted to the system. These observations indicate that $Ti(CO)_6$ is an extremely unstable compound which probably decomposes around 40–45 K to titanium metal and CO. Similar results were obtained for the "yellowish-red" $Ti(N_2)_6$ complex at about 40 K. However, the possibility that some $Ti(CO)_6$ or $Ti(N_2)_6$ sublimed from the optical window and was lost in the vacuum shroud cannot be dismissed on the basis of the present

study. Quadrupole mass spectrometric investigations will be required to establish clearly the gas phase stability and fate of $Ti(CO)_6$ and $Ti(N_2)_6$ during boil-off experiments.

Conclusion

The infrared and ultraviolet–visible spectroscopic evidence presented for the highest stoichiometry products of the Ti/CO and Ti/N_2 matrix reactions points emphatically to the existence of $Ti(CO)_6$ and $Ti(N_2)_6$, respectively.

The discovery of these 16-electron complexes can be considered to complete the 17- and 18-electron series $V(CO)_6/Cr(CO)_6$ and $V(N_2)_6/Cr(N_2)_6$ and moreover suggests that the metal atom route should provide a synthetic pathway to the Nb, Ta, Mo, and W analogues. Preliminary experiments with these highly refractory metals in our laboratories indicate that in practice this is indeed the case.[22]

A small molecular distortion away from regular octahedral symmetry for $Ti(CO)_6$ and $Ti(N_2)_6$ is implied from the infrared spectroscopic data. The corresponding UV–visible data, on the other hand, appear to be relatively insensitive to this molecular perturbation. The magnitude and symmetry (tetragonal or trigonal) of this distortion cannot be established from the available data. However, one can tentatively say that it is larger than that observed for $V(CO)_6$ and $V(N_2)_6$.

Acknowledgment. We gratefully acknowledge the financial assistance of the National Research Council of Canada and the Atkinson Foundation. The expert assistance of Professor A. B. P. Lever with the analysis of the electronic spectra is also gratefully appreciated.

Registry No. $Ti(CO)_6$, 61332-66-9; $Ti(N_2)_6$, 61332-67-0.

References and Notes

(1) M. T. Anthony, M. L. H. Green, and D. Young, *J. Chem. Soc., Dalton Trans.*, 1419 (1975).
(2) R. Busby, W. Klotzbücher, and G. A. Ozin, *J. Am. Chem. Soc.*, **98**, 4013 (1976).
(3) H. Huber, T. A. Ford, W. Klotzbücher, E. P. Kündig, M. Moskovits, and G. A. Ozin, *J. Chem. Phys.*, in press.
(4) E. P. Kündig, M. Moskovits, and G. A. Ozin, *Nature (London)*, **254**, 503 (1975).
(5) H. Huber, T. A. Ford, M. Moskovits, G. A. Ozin, and W. Klotzbücher, *Inorg. Chem.*, **15**, 1666 (1976).
(6) P. L. Timms, *Chem. Commun.*, 1033 (1969).
(7) E. P. Kündig and G. A. Ozin, *J. Am. Chem. Soc.*, **96**, 3820 (1974).
(8) K. J. Klabunde and H. F. Efner, *Inorg. Chem.*, **14**, 789 (1975).
(9) H. Huber, T. A. Ford, W. Klotzbücher, and G. A. Ozin, *J. Am. Chem. Soc.*, **98**, 3176 (1976).
(10) (a) W. Klotzbücher, A. B. P. Lever, and G. A. Ozin, *Inorg. Chem.*, in press; (b) T. C. DeVore, *Inorg. Chem.*, **15**, 1315 (1976).
(11) E. P. Kündig, M. Moskovits, and G. A. Ozin, *J. Mol. Struct.*, **14**, 137 (1972).
(12) M. Moskovits and G. A. Ozin, *J. Appl. Spectrosc.*, **26**, 481 (1972).
(13) G. A. Ozin and A. Vander Voet, *Acc. Chem. Res.*, **6**, 313 (1973).
(14) E. P. Kündig, M. Moskovits, and G. A. Ozin, *Angew. Chem., Int. Ed. Engl.*, **14**, 292 (1975).
(15) R. W. G. Wyckoff, "Crystal Structures", Vol. 7, Interscience, New York, N.Y., 1974, p 29.
(16) A. D. Buckingham, *Proc. R. Soc. London, Ser. A*, **248**, 1969 (1958); **255**, 32 (1960); *Trans. Faraday Soc.*, **56**, 763 (1960).
(17) L. Hanlan, H. Huber, E. P. Kündig, B. McGarvey, and G. A. Ozin, *J. Am. Chem. Soc.*, **97**, 7054 (1975).
(18) L. Hanlan, H. Huber, and G. A. Ozin, *Inorg. Chem.*, **15**, 2592 (1976).
(19) I. D. Chawla and M. J. Frank, *J. Inorg. Nucl. Chem.*, **32**, 555 (1970).
(20) C. J. Ballhausen, "Introduction to Ligand Field Theory", McGraw-Hill, New Uork, N.Y., 1962.
(21) H. B. Gray and N. A. Beach, *J. Am. Chem. Soc.*, **85**, 2922 (1963).
(22) W. Klotzbücher and G. A. Ozin, in progress.
(23) For consistency the average CO stretching frequency for the doublet splitting in CO/Ar $\simeq$ 1/10 matrices has been used in Figure 7.
(24) Weaker NN stretching modes, whose absorbances were found to be Ti concentration dependent, were observed at higher frequencies (2264/2256 cm^{-1}) than those of VI′ and moreover were found to grow in relation to those of VI′ during matrix warm-up experiments in the range 10–35 K. By analogy with the $V(CO)_6/V_2(CO)_{12}$ and $Ti(CO)_6/Ti_2(CO)_n$ systems, the 2264/2256-cm^{-1} absorptions are probably best ascribed to binuclear or higher titanium cluster dinitrogen species.
(25) The increase in $10Dq$ on passing from $V(N_2)_6$ to $Cr(N_2)_6$ is not so pronounced; see ref 10a.

Contribution No. 5447 from the Arthur Amos Noyes Laboratory of Chemical Physics, California Institute of Technology, Pasadena, California 91125

Studies of the Polarization Behavior, Temperature Dependence, and Vibronic Structure of the 23 000-cm^{-1} Absorption System in the Electronic Spectra of $Mo_2(O_2CCH_3)_4$ and Related Compounds. Emission Spectrum of $Mo_2(O_2CCF_3)_4$ at 1.3 K

WILLIAM C. TROGLER, EDWARD I. SOLOMON, IB TRAJBERG, C. J. BALLHAUSEN, and HARRY B. GRAY*[1]

Received October 17, 1976 AIC607332

The 23 000-cm^{-1} absorption band in the electronic spectrum of $Mo_2(O_2CCH_3)_4$ is primarily polarized perpendicular to the metal–metal axis. Rich vibronic structure is observed for this absorption system in the spectra of $Mo_2(O_2CCH_3)_4$, $Mo_2(O_2CCD_3)_4$, $Mo_2(O_2CCF_3)_4$, and $Mo_2(O_2CH)_4$ at 15 K. Analysis of the temperature dependence of the hot bands in the spectrum of $Mo_2(O_2CCF_3)_4$ has established that the transition is vibronic, being allowed primarily by an a_{2u}(MoMoO) bending vibration ($\sim$190 cm^{-1}). Interpretation of the vibronic structure in the spectrum of $Mo_2(O_2CCH_3)_4$ suggests that the 0–0 transition is split by 275 cm^{-1} into x- and y-polarized components. This splitting, which is much larger in $Mo_2(O_2CCF_3)_4$, correlates with departures from ideal D_{4h} symmetry that are evident from crystal structure determinations. A dominant progression in the MoMo totally symmetric stretch is observed on each of several vibronic origins in the spectrum of $Mo_2(O_2CCH_3)_4$. Franck–Condon analysis demonstrates that a 0.1-Å elongation of the MoMo bond occurs in the excited state. From the lowest energy vibronic origin in $Mo_2(O_2CCF_3)_4$, an estimate of 90 cm^{-1} for the metal–metal torsional frequency is obtained. Structured emission is observed for $Mo_2(O_2CCF_3)_4$ at 1.3 K ($\tau \approx 2$ ms). The emission origin lies 1800 cm^{-1} lower than that of the absorption system. The results are consistent with the assignment of the absorption band to the orbitally forbidden, metal-localized transition $^1A_{1g} \rightarrow {}^1E_g$ ($\delta \rightarrow \pi^*$) and the emission to the corresponding triplet $\rightarrow$ singlet transition.

Introduction

It is now well established that the low-energy absorption system of moderate intensity ($\epsilon \sim 10^3$) in the electronic spectra of $Re_2Cl_8^{2-}$, $Re_2Br_8^{2-}$, $Re_2Cl_6[P(C_2H_5)_3]_2$, and $Mo_2Cl_8^{4-}$ is attributable to the electric dipole allowed transition $\delta \rightarrow \delta^*$ ($^1A_{1g} \rightarrow {}^1A_{2u}$).[2-4] By contrast, spectra of $Mo_2(O_2CR)_4$ (R $\neq$ aromatic) exhibit only a weak low-energy band ($\epsilon \sim 10^2$) which peaks at about 440 nm ($\sim$23 000 cm^{-1}).[5] Recently, Cotton, Martin, and co-workers have examined the polarized crystal spectra of $Mo_2(O_2CCH_2NH_3)_4(SO_4)_2 \cdot 4H_2O$[6] and $Mo_2(O_2CH)_4$.[7] Although a firm assignment of the weak system was not made, it was shown[6] conclusively that the transition in question in the $Mo_2(O_2CR)_4$-type compounds could not be $\delta \rightarrow \delta^*$ ($^1A_{1g} \rightarrow {}^1A_{2u}$).

We have examined the polarized spectra of a crystal of $Mo_2(O_2CCH_3)_4$ as well as films of $Mo_2(O_2CCD_3)_4$,